RSC Advances

ROYAL SOCIETY OF CHEMISTRY

www.rsc.org/advances

RSC Advances

ARTICLE

Liquid-crystalline perylene tetracarboxylic bisimide derivative bearing trisiloxan-2-yl moieties: Influence on mesomorphic property and electron transport

Received 00th January 20xx,
Accepted 00th January 20xx

DOI: 10.1039/x0xx00000x

www.rsc.org/

Masahiro Funahashi,[a] Nozomi Takeuchi[a] and Akinari Sonoda[b]

Mesomorphic and electron transport properties are compared for liquid-crystalline (LC) perylene tetracarboxylic bisimide (PTCBI) derivatives bearing linear disiloxane and trisiloxane chains, as well as bis(trimethylsiloxanyl)methylsilyl (trisiloxan-2-yl) groups. In contrast to alkyl-substituted analogues, the PTCBI derivative bearing bulky trisiloxan-2-yl moieties exhibits a more ordered columnar phase and higher electron mobility, compared to that bearing linear trisiloxane chains. In spite of the bulkiness, the trisiloxan-2-yl moieties do not inhibit closed π–π stacking within the columnar aggregates. Therefore the electron mobility in the ordered columnar phase of the compound bearing the branched trisiloxan-2-yl moieties was 0.05 $cm^2V^{-1}s^{-1}$ at room temperature and it exceeded 0.1 $cm^2V^{-1}s^{-1}$ at 120 °C.

Introduction

Liquid crystals have been applied to displays, utilizing their optical anisotropy. New electronic and optical functions produced by integration of π-conjugated moieties in liquid-crystalline (LC) systems have recently been investigated. LC semiconductors consist of extended π-conjugated systems and alkyl side chains. They exhibit high carrier mobilities exceeding 0.1 $cm^2V^{-1}s^{-1}$.[1] Efficient electronic carrier transports have been observed in the columnar[2] and smectic phases.[3] Solution-processable LC semiconductors have been applied to field-effect transistors[4], polarized electroluminescence devices[5] and solar cells[6] were reported. LC semiconductors are soft and suitable for flexible devices compared to crystalline semiconductors.[4e]

Recently various LC molecules consisting of incompatible parts have been reported. Such LC molecules form various nanostructured LC phases.[7] The significant factor to form the LC phases of these molecules is microsegregatioin on nanometer scale or nanosegregation between the incompatible moieties while thermal motion of alkyl chains moderately weakens strong π–π interaction in conventional LC materials.[8]

Perylene tetracarboxylic bisimide (PTCBI) derivatives are typical n-type organic semiconductors and LC analogues bearing alkyl chains have been reported.[9] Space charge limited current measurement, microwave absorption method, and field effect transistors revealed high electron mobilities over 0.1 $cm^2V^{-1}s^{-1}$ in their LC phases. However, time-of-flight (TOF) measurements revealed low drift mobilities of electrons in the LC alkylated PTCBI derivatives.[10]

We have recently reported nanosegregated LC semiconductors consisting of perylene tetracarboxylic bisimide (PTCBI) cores and oligosiloxane chains.[11] The PTCBI derivatives bearing four oligosiloxane moieties exhibit columnar phases at room temperature and high electron mobilities[11,e,f] while the compounds bearing two oligosiloxane units show lamellar structures.[11] In these LC phases, element-block type organic/inorganic hybrid structures were formed by nanosegregation.[7f] Unlike conventional LC semiconductors, nanosegregation between the flexible oligosiloxane chains and rigid π–conjugated systems is a main driving force to form LC columnar aggregates. In conventional LC materials, alkyl side chains are restricted to linear ones in principle. Branched alkyl chains often inhibit molecular packing and destabilize mesophases because of their bulkiness.[12]

In this study, we report stabilization of the columnar phase and enhancement of electron transport in the PTCBI derivative **1** bearing bulky bis(trimethylsiloxannyl)methylsilyl (trisioxan-2-yl) groups, as shown in Scheme 1. Scheme 2 shows molecular structures of PTCBI derivatives **2** and **3** bearing four oligosiloxane moieties which were previously reported.[11a,b] Compared to a PTCBI derivative **2** bearing four linear trisiloxane chains to exhibit a disordered columnar phase, the compound **1** bearing four trisiloxan-2-yl moieties exhibit ordered columnar phase and the electron mobility exceeds 0.1 $cm^2V^{-1}s^{-1}$ at 120 °C although these two compounds are structural isomers. The electron mobility of compound **1** at elevated temperatures is larger than that of PTCBI derivative **3** bearing four disiloxane chains which occupy smaller volume.

LC materials bearing silsesquioxane, linear disiloxane and trisiloxane chains have been studied.[13] Recently a few

[a] Department of Advanced Materials Science, Faculty of Engineering, Kagawa University, 2217-20 Hayashi-cho, Takamatsu, Kagawa 761-0396 Japan. Fax: (+81)-87-864-2411; Tel: (+81)-87-864-2411; E-mail: m-funa@eng.kagawa-u.ac.jp
[b] Health Research Institute, National Institute of Advanced Industrial Science and Technology, 2217-14 Hayashi-cho, Takamatsu, Kagawa 761-0395, Japan.
See DOI: 10.1039/x0xx00000x

conjugated polymers bearing oligosiloxane moieties have been reported.[14a,b] Only few calamitic LC materials bearing the trisiloxane-2-yl unit were synthesized so far,[14c,d] but it has not been considered as side chains of discotic LC molecules or low molecular weight organic semiconductors.

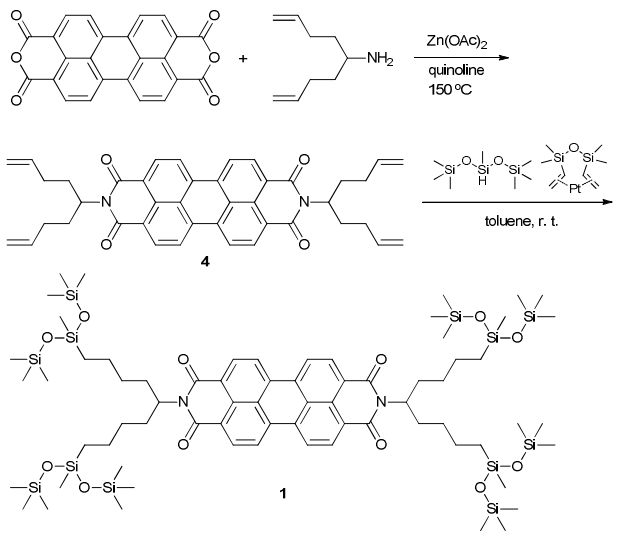

Scheme 1 Synthetic route of a PTCBI derivative **1** bearing trisiloxan-2-yl groups

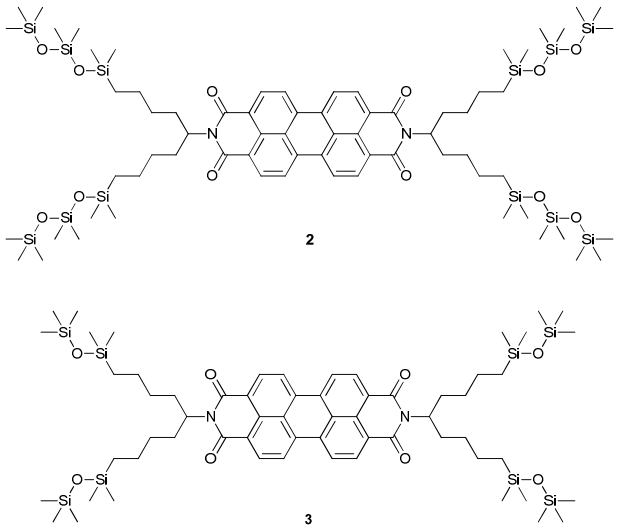

Scheme 2 Molecular structures of PTCBI derivatives bearing linear oligosiloxane chains

Experimental

Characterization of LC phases

The mesomorphic properties of the PTCBI derivatives were studied by differential scanning calorimetry (DSC), polarizing optical microscopy, and X-ray diffraction (XRD). A polarizing optical microscope (Olympus DP70) equipped with a hand-made hot stage was used for the visual observation of the optical textures. DSC measurements were conducted on a NETZSCH DSC 204 Phoenix. XRD measurements were carried out on a Rigaku Rapid II diffractometer by using Ni-filtered CuKα radiation.

Measurement of electron mobility

Electron mobilities were measured by the time-of-flight (TOF) method.[15] A liquid crystal cell was fabricated by combining two ITO-coated glass plates. The cell was placed on a hot stage and heated at 125 °C. LC samples were melted and filled into the cell via a capillary action. The cells were cooled at a rate of 0.1 degree/min. The liquid crystal cell was placed on the hot stage of the TOF setup. A DC voltage was applied to the cell using an electrometer (ADC R8252) and a pulse laser was illuminated on the cell. The excitation source was the third harmonic generation of a Nd:YAG laser (Continuum MiniLite II, wavelength = 356 nm, pulse duration = 2 ns) and the induced displacement currents were recorded using a digital oscilloscope (Tektronics TDS 3044B) through a serial resistor.

Synthesis of materials

All the ^{1}H and ^{13}C NMR spectra were recorded on a Varian UNITY INOVA400NB spectrometer. FT-IR measurements were conducted on a JASCO FT/IR-660 Plus spectrometer. Bis(trimethylsiloxanyl)methylsilane and the Karstedt catalyst were purchased from Gelest Inc. Tetrahydrofuran, toluene, and dimethoxyethane were obtained from Wako Pure Chemical Industries and were used without purification. Silica gel was purchased from Kanto Chemicals.

The LC PTCBI derivative was synthesized as shown in Scheme 1. Perylene tetracarboxylic anhydride was converted to alkenyl-substituted perylene tetracarboxylic bisimide **4**. Bis(trimethylsiloxy)methylsilane were reacted with the terminal double bonds of the side chains using the Karstedt catalyst[16] in toluene at room temperature, producing compounds **1**.

***N-N'*-bis{1,9-di(1,1,1,2,3,3,3-heptamethyl-1,3,5-trisiloxan-3-yl)nonane-5-yl} perylene-3,4,9,10-tetracarboxylic bisimide (1)**

N-N'-bis(1,9-nonane-5-yl)perylene-3,4,9,10-tetracarboxlic bisimide (4) 1.18 g (1.9 mmol) and bis(trimethylsiloxanyl)methylsilane 2.09 g (10.2 mmol) were dissolved in toluene (30 ml) and 10 μl of Karstedt catalyst (1,3-divinyl-1,1,3,3-tetramethyldisiloxane platinum (0), 2.1 atom%, xylene solution) was added to the reaction mixture. The solution was stirred at room temperature for two hours. The solvent was evaporated and the resultant red residue was purified by a column chromatography (elutant: *n*-hexane and ethyl acetate (10:1)). The crude product was dissolved in dichloromethane and the solution was poured into methanol. The red precipitates were filtered. Red powder (0.965 g, 0.66 mmol) was obtained in the yield of 36 %. ^{1}H NMR (400 MHz, $CDCl_3$): δ = 8.67 (d, br, 4H, J = 8.4 Hz), 8.59 (d, 4H, J = 8.4 Hz), 5.17 (tt, 2H, J = 9.2, 6.0 Hz), 2.18-2.30 (m, 4H) , 1.80-1.91 (m, 4H), 1.19-1.42 (m, 16H), 0.40 (dd, 8H, J = 9.2, 6.8 Hz), 0.02 ppm (s, 72H), -0.07 ppm (s, 12H); ^{13}C NMR (100 MHz, $CDCl_3$): δ = 159.8, 130.7, 128.1, 127.4, 125.9, 122.7, 119.2, 51.1, 28.5, 26.9, 19.4, 13.9, -1.9, -4.1 ppm; IR (ATR) : ν = 2958, 1699, 1659, 1595, 1579, 1405, 1338, 1251, 1037, 834,

808, 781, 752 cm^{-1}; Exact Mass: 1522.65; Molecular Weight: 1524.78; m/z [MH^+]: 1526.41, 1525.41, 1527.42, 1528.42, 1524.41, 1523.39, 1529.4; Elemental Analysis (%) calculated for $C_{70}H_{126}N_2O_{12}Si_{12}$: C, 55.14; H, 8.33; N, 1.84; O, 12.59; Si, 22.10; found: C, 55.20; H, 8.50.

Compounds **2** and **3** which bearing linear 1,1,1,3,3,5,5-heptamthyl-1,3,5-trisiloxane and 1,1,1,3,3-pentamethyl-1,3-disiloxane chains (Scheme 2) were prepared from compound **4** by the procedure reported previously.[11a,b] It should be noted that compound **2** is a structural isomer of compound **1**.

Results and discussion

Characterization of the mesophase of compound 1

As shown in Figure 1, compounds **1** and **2** exhibit single enantiotropic LC phases below 122.5 ºC and 62.5 ºC, respectively. They do not crystallize when they are cooled to -100 ºC. As discussed later, the columnar phases of compounds **1** and **3** are ordered columnar phases while compound **2** exhibits a columnar disordered phase. Phase transition enthalpies of compounds **1** and **3** are larger than that of compound **2**. It is reasonable because remarkable thermal motion inhibits closed molecular aggregation in the LC phase, resulting in the disordered columnar phase of compound **2**. Glass transitions originated from the freeze of the thermal motion of the oligosiloxane chains are observed around -60 ºC for compounds **1** and **3** and -80 ºC for compound **2**. Compared to the longer trisiloxane chains of compound **2**, mobility of the 2-siloxanyl moieties should be comparable to that of the disiloxane chains of compound **3**.

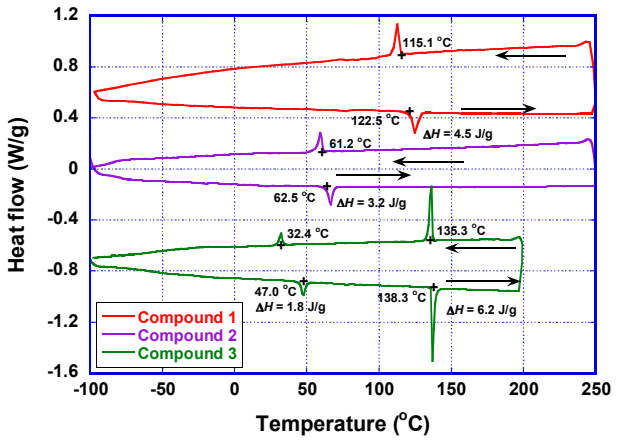

Figure 1 DSC thermograms of compound **1**-**3** at heating and cooling rate of 10 K/min.

Table 1 Phase transition temperatures (enthalpy / Jg^{-1}) of compounds **1**-**3**

Compound **1**	Glassy Col_{ro} -63 ºC Col_{ro} 122.5 ºC (4.5) Iso
Compound **2**	Glassy Col_{ro} -82 ºC Col_{hd} 62.5 ºC (3.2) Iso
Compound **3**	Glassy Col_{ro} -58 ºC Col_{ro} 47.0 ºC (1.8) Col_{ho} 138.3 ºC (6.2) Iso

Col_{ro}: columnar rectangular ordered phase; Col_{ho}: columnar hexagonal ordered phase; Col_{hd}: columnar hexagonal disordered phase; Iso: isotropic phase

Figure 2(a) exhibits a polarizing optical micrograph of compound **1** at room temperature. By leaving the sample at 122 ºC, the sizes of the LC domains exceeded several hundred μm. There were two kinds of domains with high and low birefringence. LC nuclei with rectangular shapes grew to be the high-birefringent domains at the phase transition temperature between the isotropic and the LC phases, as shown at the upper left of Figure 2(a). In the domains, the columnar aggregates of compound **1** align parallel to the surface of the substrate. In contrast, the low-birefringent domains are formed via elongated hexagonal dendritic LC droplets, suggesting a pseudo-hexagonal columnar order, as shown at the centre of Figure 2(a). In the domains, the columnar aggregates are perpendicular to the surface of the substrate. The non-zero birefringence of the domains should be attributed to the pseudo-hexagonal columnar arrangement, i. e., rectangular lattice, although the domains should be non-birefringent in a completely hexagonal columnar arrangement.

Figure 2(b) exhibits a polarizing optical micrograph of compound **2** at room temperature. Dark homeotropic domains indicate that columnar aggregates orient perpendicular to the surface of the substrate. Domains with a defect line were observed, indicating the presence of bent columnar aggregates. This suggests that the columnar aggregates are soft and flexible compared to those of compound **1**. As shown in Figure 2(a), no domains with a defect line derived from the bent structures of columnar aggregates were observed for compound **1**. For compound **3**, non-birefringent hexagonal dendritic textures were observed below the phase transition temperature between the isotropic and hexagonal ordered phases, and defect lines were formed in the rectangular ordered columnar phase at room temperature, as reported previously.[11b]

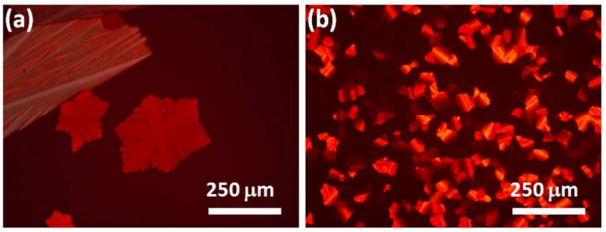

Figure 2 Polarizing optical micrographs of (a) growing LC domains of compound **1** at 122 ºC and (b) LC domains of compound **2** at room temperature

Figure 3 exhibits X-ray diffraction patterns of compound **1** and **2** at room temperature. For compound **1**, many diffraction peaks derived from a rectangular columnar arrangement with the symmetry of *P2m* were observed. Diffraction peaks at 3.74º, 6.19º, 7.51º, 8.72º, 9.47º, 10.38º, 12.08º, 12.81º, 14.28º, 14.95º, 17.64º, and 23.29º are assigned to (100), (120), (200), (220), (040), (230), (320), (240), (250), (410), (440), and (620) diffraction planes. The lattice parameters calculated from the (100) and (010) diffractions are 25.1 Å and 35.6 Å, respectively. In a conventional rectangular columnar phase, LC molecules usually tilt to the columnar axis and one lattice parameter is shorter than the size of the disk-like molecules. In this columnar phase of compound **1**, the LC molecules do not tilt to the columnar axis. The shorter (100) lattice parameter than the

extended length of the molecule of compound **1**, 34 Å should be attributed to the interdigitation of the trisiloxan-2-yl groups. In contrast, (010) lattice parameter is comparable to the extended length of the molecule of compound **1**. In this direction, the interdigitation is not remarkable. In addition, it should be noted that a diffraction peak at 25.52º derived from the π-π stacking in the columnar aggregates is observed. This peak is assigned to (001) diffraction plane and the π-π stacking distance within the columnar aggregates was estimated to be 3.49 Å. This columnar phase of compound **1** is identified to be a columnar rectangular ordered phase.

In contrast to compound **1** exhibiting ordered columnar phase, compound **2** exhibits a disordered columnar phase. In the X-ray diffraction pattern, only two weak and ambiguous peaks were observed other than a relatively strong peak at 3.71º, which is originated to a (100) diffraction plane. The weak peaks at 6.28º and 7.54º are assigned to (110) and (200) planes. The lattice constant calculated from the diffraction peaks are 23.8 Å, 14.07 Å, and 7.54 Å. The ratio of the constants was 1: 1/√3:1/2 and no peak derived from the long-range order of the molecular position within the columnar aggregates was observed. Therefore the LC phase is identified to be a hexagonal columnar disordered phase. The lattice spacing corresponding to the (100) diffraction plane is 23.8 Å, which is much shorter than the fully extended length of the molecule of compound **2**, 37 Å. This result indicates interdigitation of the linear trisiloxane chains of compound **2** as in the columnar phase of compound **1**.

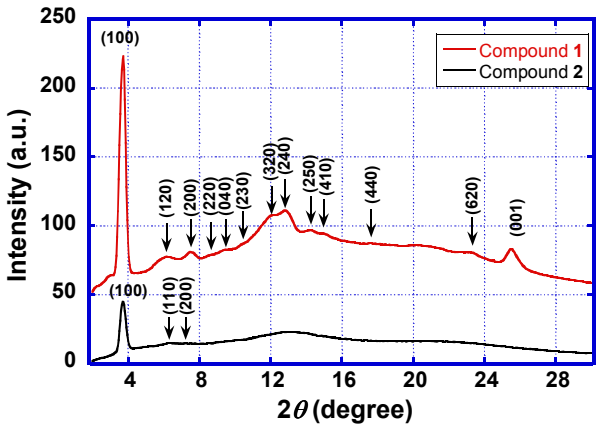

Figure 3 X-ray diffraction patterns of compounds **1**-**2** at room temperature

The (100) diffraction lattice parameters of the columnar phases of compounds **1** and **2** are comparable. This result implies disordered conformation of the linear trisiloxane chains of compound **2** in the columnar phase, in addition to the interdigitation of the trisiloxane chains. However, the molecular aggregation state within columns is remarkably influenced by the change in the position of the trisiloxane chain connected to the alkyl chains. In the columnar phase of compound **2**, the positional order within the columnar aggregates disappears while long range order of the molecular positions exists within the columnar aggregates of compound **1**. Thermal motion of the trisiloxan-2-yl moieties of compound **1** should be restricted, compared to the linear trisiloxane chains of compound **2**.

Compound **3** exhibit columnar hexagonal ordered and rectangular ordered phases as reported previously.[10b] The lattice parameter estimated from the (100) diffraction plane in the columnar phase of compound **3** at room temperature is 21.8 Å. This value is shorter than that of compound **1**. Compound **3** also have positional order of the LC molecules within columnar aggregates based on π-π stacking as compound **1**. Comparing compounds **1** and **3**, the addition of one trimethylsiloxy unit to the 1-position of the disiloxane chains of compound **3** does not influence the π–π stacking within the columnar aggregates of compound **1**. In the direction of the columnar axes, π-conjugated cores form closed π–π stacking structure in the columnar phases of compounds **1** and **3** because the oligosiloxane moieties avoid their confliction by the construction of the staggered stacking structures.

Temperature-dependence of the lattice parameters

Figure 4 exhibits lattice constants determined from (100) and (001) diffraction planes. The former and latter values correspond to the intercolumnar and the intracolumnar π–π stacking distances, respectively.

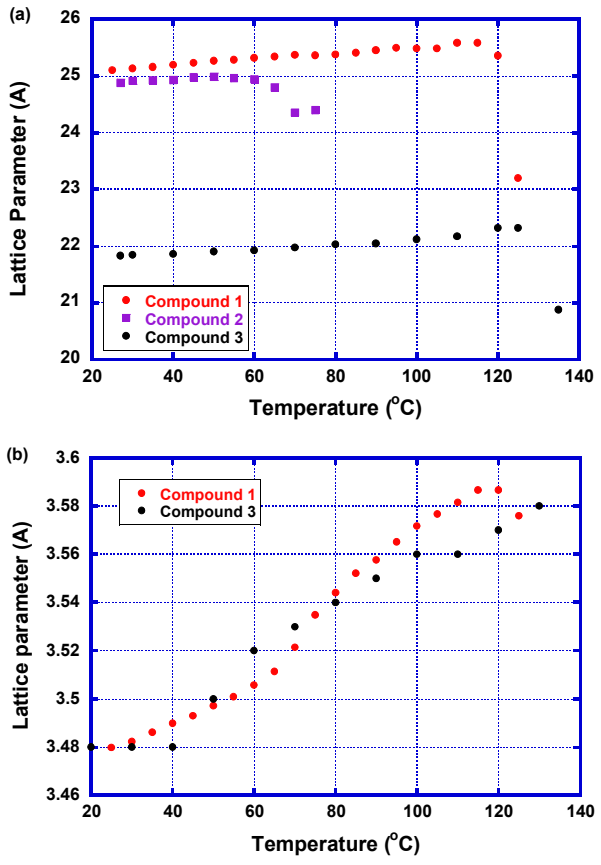

Figure 4 Lattice constants as a function of the temperature (a) (100) plane (intercolumnar distance) and (b) (001) plane (π–π stacking distance within the columnar aggregates) for compounds **1** and **3**

Compared to compound **3** bearing four disiloxane chains, compounds **1** and **2** have larger intercolumnar distances. It is reasonable because linear trisiloxane chains of compound **2** and trisiloxan-2-yl groups of compound **1** occupy larger spaces than the disiloxane chains of compound **3**. Comparing compound **1** with compound **2**, the intercolumnar distance of compound **1** bearing four trisiloxan-2-yl moieties is greater than that of compound **2**. This result indicates that linear trisiloxane chains of compound **2** interdigitate remarkably, compared to the columnar phase of compound **1**. In other words, trisiloxan-2-yl moieties of compound **1** occupy more volume than linear trisiloxane chains of compound **2**.

The temperature-dependence of the lattice parameters determined from the (100) diffraction plane, which correspond to the intercolumnar distances for compounds **1** and **3** exhibit the same dependence. They gradually increase with an increase in the temperature as shown in Figure 4(a). This tendency should be attributed to the increase in the thermal motion of the oligosiloxane side chains with the temperature. In the disordered columnar phase of compound **2**, the lattice parameter decreases near the phase transition temperature to the isotropic phase. This should be interpreted as pre-transitional behaviour before the melt of the columnar aggregates.

The lattice parameters determined from the (001) diffraction plane indicate the π–π stacking distances in the columnar aggregates of compounds **1** and **3**. For both compounds, the lattice parameters increase with the temperature. The thermal motion of the oligosiloxane chains expands the π–π stacking distances in the columnar phases of compounds **1** and **3**.

The dominant factor to determine the intercolumnar distance is volume of the oligosiloxane moieties. The intercolumnar distance in the ordered columnar phase of compound **1** is greater than that of the disordered columnar phase of compound **2**. The π–π stacking distance should depend on the freedom of the thermal motion of the oligosiloxane moieties. Compound **1** forms ordered columnar phase in which the π-conjugated cores stack closely and periodically as compound **3** exhibits the ordered columnar phase. However, compound **2** exhibits the disordered columnar phase due to the thermal motion of linear trisiloxane chains.

Characterization of electron transport in the columnar phase

Electron mobility in the columnar phase of compound **1** was determined by a time-of-flight technique. Figure 5(a) exhibits transient photocurrent curves for electrons in the columnar phase of compound **1** at room temperature. Although periodical noises derived from excitation laser pulse are observed in the time ranges shorter than 0.1 μs, non-dispersive transient photocurrent curves are obtained for the electrons at room temperature. The electron mobility is 5×10^{-2} $cm^2V^{-1}s^{-1}$, which is independent of the electric field as shown in Figure 5(b).

The electron mobility in the columnar phase of compound **1** is close to that in the ordered columnar phase of compound **3**.[11b] It is two orders of magnitude higher than that in the disordered columnar phase of compound **2**.[11a] This field-independent mobility indicates small energetic disorder in the columnar phase of compound **1**, as compared to amorphous organic semiconductors. In amorphous organic semiconductors, carrier mobility exhibits positive field-dependence, due to field-assisted charge carrier hopping.[17]

Figure 6 exhibits the electron mobilities in the columnar phases of compounds **1-3** as a function of the temperature. Between room temperature and 120 ºC, the electron mobility for compound **1** gradually increases with the temperature while it decreases with the temperature in the columnar phase of compound **3**. The electron mobility in the disordered columnar phase of compound **2** which is a structural isomer of compound **1** is two orders of magnitude lower than that of compound **1**. Unlike the ordered columnar phases of compounds **1** and **3**, the columnar phase of compound **2** is a disordered columnar phase, in which the electron hopping is not efficient due to the loose molecular aggregation in the columnar phase. The appearance of the disordered columnar phase in compound **2** should be attributed to the bulkiness and freedom of the conformation of the linear trisiloxane chains compared to those of the disiloxane chains of compounds **1** and **3**.

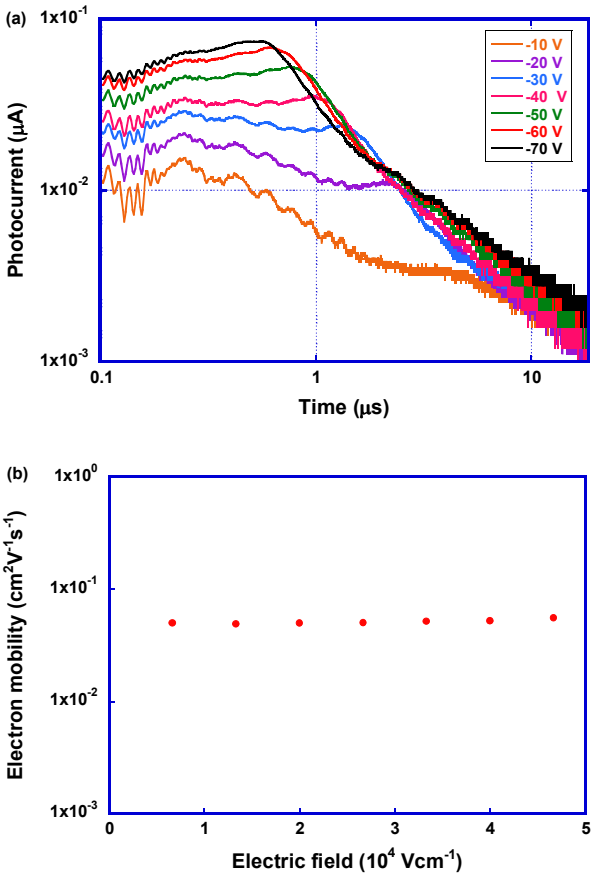

Figure 5 Transient photocurrent curves for electrons in the columnar phase of compound **1** at 30 °C. The sample thickness is 15 μm, and the wavelength of the excitation laser pulse is 355 nm. (b) Electron mobility in the columnar phase of compound **1** as a function of the electric field at 30 °C.

Comparing the electron mobilities in the columnar phases of compounds **1** and **3**, the π–π stacking distances are almost same at room temperature. However, the electron mobility of

compound **3** is twice higher than that of compound **1**. The temperature-dependences of these electron mobilities in the columnar phases of compounds **1** and **3** are opposite. For compound **1**, the electron mobility increases with an increase in the temperature while it decreases with an increase in the temperature for compound **3**. Above 80 ºC, the electron mobility in the columnar phase of compound **1** is higher than that of compound **3**.

Carrier transport characteristics in the LC phases below room temperature have been described by the small polaron[18] or disorder[19] models which are applied to organic amorphous semiconductors.[17] Analysis based on one-dimensional disorder model revealed the energetic disorder of ca. 50 meV in the ordered columnar phases of the PTCBI derivatives bearing four disiloxane chains.[11e] In contrast, temperature- and field-independent carrier mobilities are often observed in the smectic and columnar phases above room temperature.[2-3] In this temperature region, most of the charge carriers are thermally excited to the transport level and the temperature-dependence of carrier mobilities in the LC systems is strongly influenced by the dynamic nature of the LC states.[11e]

Assuming the electron mobility of 0.1 $cm^2V^{-1}s^{-1}$ and electric field of 10^4 Vcm^{-1}, the hopping time is estimated to be several ps, which is much shorter than the time scale of molecular motion in columnar phases. However, the columnar structures are disordered by the thermal motion of the side chains. Thermal activation in the charge carrier hopping process causes positive temperature-dependence of the mobilities while dynamic thermal fluctuation of the LC structures tends to decrease the mobilities. The temperature-dependence of carrier mobilities is determined by the balance between the two factors. This is quite different from the hopping transport in organic 'solid' semiconductors, in which carrier mobilities increase with an increase in the temperature.[17]

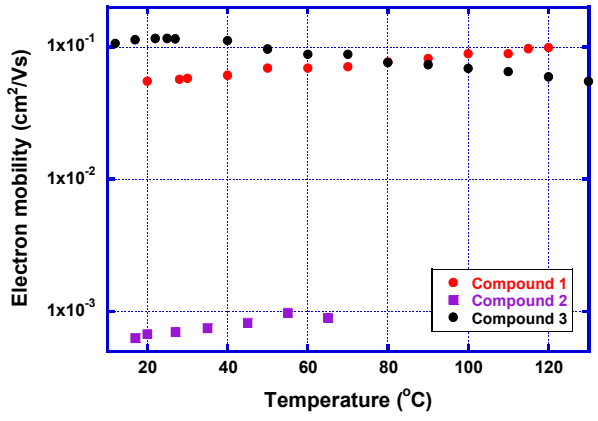

Figure 6 Electron mobility in the columnar phases of compounds **1-3** as a function of the temperature

As shown in Figure 4(b), due to thermal fluctuation of the columnar aggregates, π–π stacking distances increase with an increase in the temperature in the columnar phases of both compounds **1** and **3**. This tendency acts to decrease the electron mobilities with the temperature. However, thermal activation of the intermolecular charge transfer is dominant over this effect in the columnar phase of compound **1**. In contrast, the thermal fluctuation effect is remarkable compared to the effect of the thermal activation in the charge carrier hopping in the columnar phase of compound **3**.

The dominant factor to determine the carrier mobility in columnar phases is intermolecular π-orbital overlap which is decreased by the expansion of the π-π stacking distance within the columnar aggregates. In addition, molecular mutual rotation around the columnar axes[18e] and sliding motion of the π-conjugated cores in the direction perpendicular to the columnar decrease the intermolecular π-orbital overlap.

The trisiloxan-2-yl moieties of compound **1** are more bulky than disiloxane chains of compound **3**. As a result, the interdigitation of the trisiloxan-2-yl moieties in the ordered columnar phase of compound **1** is not remarkable compared to that for compound **3**, as shown in Figure 4(a). This tendency should suppress thermal motion of the π-conjugated core perpendicular to the columnar axes as well as molecular mutual rotation around the columnar axes in the LC phase of compound **1**. For compound **1**, the thermal expansion of the columnar aggregates along the columnar axes decreases intermolecular π-orbital overlap, but this effect is cancelled by the thermal activation in the charge carrier hopping process. In the columnar phase of compound **3**, not only the thermal expansion of the columnar aggregates along the columnar axes but also positional disorder of the π-conjugated cores caused by mutual rotation and sliding motion of the π-conjugated cores should lower the electron mobility with an increase in the temperature.

Conclusions

Mesomorphic structures and electron transport characteristics in the columnar phases of PTCBI derivatives bearing oligosiloxane chains are compared. Trisiloxan-2-yl groups enhance the formation of the ordered columnar aggregates and electron transfer. Compound **1** exhibits an ordered columnar phase in spite of its bulky trisiloxan-2-yl side chains. In the ordered columnar phase of compound **1**, the interdigitation of the trisiloxan-2-yl groups is not so remarkable as that of compound **2** and **3** which have linear oligosiloxane chains. The electron mobility in the ordered columnar phase of compound **1** is 0.05 $cm^2V^{-1}s^{-1}$ and it increases with the temperature. Above 80 ºC, the electron mobility is higher than that of compound **3**. The value exceeds 0.1 $cm^2V^{-1}s^{-1}$ at 120 ºC. The temperature dependence of the electron mobility in the columnar phases is determined by the balance of thermal activation effect in the electron hopping process and thermal fluctuation of the columnar aggregates. The thermal fluctuation of the columnar structure includes the thermal expansion of the π-π stacking distance within the columnar aggregates and the sliding motion of the π-conjugated cores in the direction perpendicular to the columnar axes. The introduction of these oligosiloxane moieties is effective to stabilize the LC phases of not only the PTCBI

derivatives but also other mesogenic compounds. The detailed study is in progress.

Acknowledgements

This study was financially supported by the Japan Security Scholarship Foundation, the Ogasawara Foundation, a Grant-in-Aid for Scientific Research on Innovative Areas (Coordination Programming, no. 24108729 and Element-Block Polymers, no. 25102533) from the Ministry of Education, Culture, Sports, Science and Technology (MEXT), a Grant-in-Aid for Scientific Research (B) (no. 22350080) from the Japan Society for the Promotion of Science (JSPS), the Iwatani Naoji Foundation, the Asahi Glass Foundation, and the Murata Science Foundation. The authors thank T. Kusunose at Kagawa University for help with the DSC measurements.

Notes and references

1 (a) W. Pisula, M. Zorn, J. Y. Chang, K. Müllen, R. Zentel, *Macromol. Rapid Commun*., 2009, **30**, 1179-1202. (b) Y. Shimizu, K. Oikawa, K. Nakayama, D. Guillon, *J. Mater. Chem*. 2007, **17**, 4223-4229. (c) M. O'Neill, S. M. Kelly, *Adv. Mater*., 2011, **23**, 566-584. (d) M. Funahashi, H. Shimura, M. Yoshio, T. Kato, *Structure and Bonding*, 2008, **128**, 151-179. (e) M. Funahashi, T. Yasuda, T. Kato, *Handbook of Liquid Crystals* 2nd Ed. Wiley-VCH, 2014, **8**, 675-708. (f) A. Seki, M. Funahashi, *Heterocycles*, 2015, **91**, in press.

2 (a) D. Adam, F. Closs, T. Frey, D. Funhoff, D. Haarer, H. Ringsdorf, P. Schuhmacher, K. Siemensmeyer, *Phys. Rev. Lett*., 1993, **70**, 457-460. (b) N. Boden, R. J. Bushby, J. Clements, B. Movaghar, K. J. Donovan, T. Kreouzis, *Phys. Rev. B*, 1995, **52**, 13274-13280. (c) A. M. van de Craats, J. M. Warman, A. Fechtenkötter, J. D. Brand, M. A. Harbison, K. Müllen, *Adv. Mater*., 1999, **11**, 1469-1472. (d) M. Ichihara, A. Suzuki, K. Hatsusaka, K. Ohta, *Liq. Cryst*., 2007, **34**, 555-567. (e) K. Ban, K. Nishikawa, K. Ohta, A. M. van de Craats, J. M. Warman, I. Yamamoto, H. Shirai, *J. Mater. Chem*., 2001, **11**, 321-331. (f) A. Demenev, S. H. Eichhorn, T. Taerum, D. Perepichka, S. Patwardhan, F. C. Grozema, L. D. A. Siebbeles, *Chem. Mater*., 2010, **22**, 1420-1428. (g) J. Simmerer, B. Glüsen, W. Paulus, A. Kettner, P. Schuhmacher, D. Adam, K.-H. Etzbach, K. Siemensmeyer, J. H. Wendorf, H. Ringsdorf, D. Haarer, *Adv. Mater*., 1996, **8**, 815-819.

3 (a) M. Funahashi, J. Hanna, *Phys. Rev. Lett*., 1997, **78**, 2184-2187. (b) M. Funahashi, J. Hanna, *Appl. Phys. Lett*., 2000, **76**, 2574-2576. (c) M. Funahashi, J. Hanna, *Adv. Mater*., 2005, **17**, 594-598. (d) K. Oikawa, H. Monobe, J. Takahashi, K. Tsuchiya, B. Heinrich, D. Guillon, Y. Shimizu, *Chem. Commun*., 2005, 5337-5339. (e) A. Matsui, M. Funahashi, T. Tsuji, T. Kato, *Chem. Eur. J*., 2010, **16**, 13465-13472. (f) H. Aboubakr, M.-G. Tamba, A. K. Diallo, C. Videlot-Ackermann, L. Belec, O. Siri, J.-M. Raimundo, G. H. Mehl, H. Brisset, *J. Mater. Chem*., 2012, **22**, 23159-23168. (g) M. Funahashi, F. Zhang, N. Tamaoki, J. Hanna, *ChemPhysChem*, 2008, **9**, 1465-1473. (h) M. Funahashi, T. Ishii, A. Sonoda, *ChemPhysChem*, 2013, **14**, 2750-2758.

4 (a) A. J. J. M. van Breemen, P. T. Herwig, C. H. T. Chlon, J. Sweelssen, H. F. M. Schoo, S. Setayesh, W. M. Hardeman, C. A. Martin, D. M. de Leeuw, J. J. P. Valeton, C. W. M. Bastiaansen, D. J. Broer, A. R. Popa-Merticaru, S. C. J. Meskers, *J. Am. Chem. Soc*., 2006, **128**, 2336-2345. (b) M. Funahashi, F. Zhang, N. Tamaoki, *Adv. Mater*., 2007, **19**, 353-358. (c) W. Pisula, A. Menon, M. Stepputat, I. Lieberwirth, U. Kolb, A. Tracz, H. Sirringhaus, T. Pakula, K. Müllen, *Adv. Mater*., 2005, **17**, 684-689. (d) M. Funahashi, *Polym. J*., 2009, **41**, 459-469. (e) F. Zhang, M. Funahashi, N. Tamaoki, *Org. Electr*., 2010, **11**, 363-368.

5 (a) T. Hassheider, S. A. Benning, H.-S. Kitzerow, M.-F. Achard, H. Bock, *Angew. Chem., Int. Ed*., 2001, **40**, 2060-2063. (b) M. P. Aldred, A. E. A. Contoret, S. R. Farrar, S. M. Kelly, D. Mathieson, M. O'Neill, W. C. Tsoi, P. Vla-chos, *Adv. Mater*., 2005, **17**, 1368-1372. (c) S. A. Benning, R. Oesterhaus, H.-S. Kitzerow, *Liq. Cryst*., 2004, **31**, 201-205. (d) M. W. Lauhof, S. A. Benning, H.-S. Kitzerow, V. Vill, F. Scheliga, E. Thorn-Csányi, *Synth. Met*., 2007, **157**, 222-227.

6 (a) T. Hori, Y. Miyake, N. Yamasaki, H. Yoshida, A. Fujii, Y. Shimizu, M. Ozaki, *Appl. Phys. Exp*., 2010, **3**, 101602. (b) W. Shin, T. Yasuda, G. Watanabe, Y. S. Yang, C. Adachi, *Chem. Mater*., 2013, **25**, 2549-2556. (c) K. Sun, Z. Xiao, S. Lu, W. Zajaczkowski, W. Pisula, E. Hanssen, J. M. White, R. M. Williamson, J. Subbiah, J. Ouyang, A. B. Holmes, W. W. H. Wong, D. J. Jones, *Nat. Commun*., 2015, **6**, 6013.

7 (a) T. Kato, T. Yasuda, Y. Kamikawa, M. Yoshio, *Chem. Commun*., 2009, 729-739. (b) M. Funahashi, *J. Mater. Chem. C*, 2014, **2**, 7451-7459; (c) T. Yasuda, H. Ooi, J. Morita, Y. Akama, K. Minoura, M. Funahashi, T. Shimomura, T. Kato, *Adv. Funct. Mater*., 2009, **19**, 411-419. (d) S. Yazaki, M. Funahashi, T. Kato, *J. Am. Chem. Soc*., 2008, **130**, 13206-13207. (e) S. Yazaki, M. Funahashi, J. Kagimoto, H. Ohno, T. Kato, *J. Am. Chem. Soc*., 2010, **132**, 7702-7708. (e) M. Yoneya, *Chem. Rec*., 2011, **11**, 66-76. (f) Y. Chujo, K. Tanaka, *Bull. Chem. Soc. Jpn*., 2015, **88**, 633–643.

8 P. G. de Gennes, J. Prost, *The Physics of Liquid Crystals*, Oxford University Press, 1992, Oxford

9 (a) H. Langhals, *Helv. Chim. Acta*, 2005, **88**, 1309-1343. (b) F. Würthner, C. R. Saha-Möller, B. Fimmel, S. Ogi, P. Leowanawat, D. Schmidt, *Chem. Rev*., 2015, **115**, in press. (c) F. Würthner, *Chem. Commun*., 2004, 1564-1579. (d) F. Würthner, C. Thalacker, S. Diele, C. Tschierske, *Chem. Eur. J.* 2001, **7**, 2245-2253. (e) Z. Chen, U. Baumeister, C. Tschierske, F. Würthner, *Chem. Eur. J*., 2007, **13**, 450-465. (f) A. Wicklein, M-A. Muth, M. Thelakkat, *J. Mater. Chem*., 2010, **20**, 8646-8652.

10 (a) C. W. Struijk, A. B. Sieval, J. E. J. Dakhorst, M. van Dijk, P. Kimkes, R. B. M. Koehorst, H. Donker, T. J. Schaafsma, S. J. Picken, A. M. van de Craats, J. M. Warman, H. Zuilhof and E. J. R. Sudhölter, *J. Am. Chem. Soc*., 2000, **122**, 11057–11066; (b) Z. An, J. Yu, S. C. Jones, S. Barlow, S. Yoo, B. Domercq, P. Prins, L. D. A. Siebbeles, B. Kippelen and S. R. Marder, *Adv. Mater*., 2005, **17**, 2580–2583; (c) V. Duzhko, E. Aqad, M. R. Imam, M. Peterca, V. Percec and K. D. Singer, *Appl. Phys. Lett*., 2008, **92**, 113312.

11 (a) M. Funahashi, A. Sonoda, *Org. Electr*., 2012, **13**, 1633-1640. (b) M. Funahashi, A. Sonoda, *J. Mater. Chem*., 2012, **22**, 25190-25197. (c) M. Funahashi, A. Sonoda, *Dalton Trans*., 2013, **42**, 15987-15994. (d) M. Funahashi, M. Yamaoka, K. Takenami, A. Sonoda, *J. Mater. Chem. C*, 2013, **1**, 7872-7878. (e) M. Funahashi, A. Sonoda, *Phys. Chem. Chem. Phys*., 2014, **16**, 7754-7763. (f) K. Takenami, S. Uemura, M. Funahashi, *RSC Advance.,* 2016, **6**, 5474-5484.

12 (a) M. J. Hollambya, T. Nakanishi, *J. Mater. Chem. C*, 2013, **1**, 6178–6183; (b) K Isoda, T. Abe, M. Funahashi, M. Tadokoro, *Chem. Eur. J*., 2014, **20**, 7232-7235; (c) M. Nuita, J. Sakuda, Y. Hirai, M. Funahashi, T. Kato, *Chem. Lett*., 2011, **40**, 412-413.

13 (a) G. H. Mehl, J. Goodby, Angew. *Chem., Int. Ed. Engl*., 1996, **35**, 2641–2643; (b) I. M. Saez, J. W. Goodby, R. M. Richardson. *Chem. Eur. J*., 2001, **7**, 2758–2764; (c) J. Newton, H. Coles, P. Hodge, J. Hannington, *J. Mater. Chem*., 1994, **4**, 869–874; (d) J. C. Roberts, N. Kapernaum, F. Giesselmann, R. P. Lemieux, *J. Am. Chem. Soc*., 2008, **130**, 13842–13843; (e) D. Apreutesei, G. Mehl, *J. Mater. Chem*., 2007, **17**, 4711–

4715; (f) A. Zelcer, B. Donnio, C. Bourgogne, F. D. Cukiernik, D. Guillon, *Chem. Mater*., 2007, **19**, 1992–2006.

14 (a) J. Mei, D. H. Kim, A. L. Ayzner, M. F. Toney and Z. Bao, *J. Am. Chem. Soc*., 2011, **133**, 20130–20133; (b) A. Mori, K. Ide, S. Tamba, S. Tsuji, Y. Toyomori, T. Yasuda, *Chem. Lett*., 2014, **43**, 640-642. (c) W.-H. Chen, W.-T. Chuang, U-S. Jeng, H.-S. Sheu, H.-C. Lin, *J. Am. Chem. Soc*., 2011, **133**, 15674–15685; (d) C. Keith, R. A. Reddy, M. Prehm, U. Baumeister, H. Kresse, J. L. Chao, H. Hahn, H. Lang, C. Tschierske, *Chem. Eur. J*., 2007, **13**, 2556–2577.

15 (a) R. G. Kepler, *Phys. Rev*., 1960, **119**, 1226-1229. (b) W. E. Spear, *J. Non-Cryst. Solid*, 1968, **1**, 197-214.

16 B. D. Karstedt, *U.S. Patent* 3,775,452, 1973.

17 (a) H. Bässler, *Phys. Status Solidi B*, 1993, **175**, 15-56. (b) M. van der Auweraer, F. C. Schryver, P. M. Borsenberger, H. Bässler, *Adv. Mater*., 1994, **6**, 199-213. (c) A. Köhler, H. Bässler, *Top. Curr. Chem*., 2012, **312**, 1-66. (d) R. Goehoorn, P. A. Bobbert, *Phys. Status Solidi A*, 2012, **209**, 2354-2377. (e) T. Nagase, K. Kishimoto, H. Naito, *J. Appl. Phys*., 1999, **86**, 5026-5035.

18 (a) M. A. Palenberg, R. J. Silbey, M. Malagoli, J.-L. Brédas, *J. Chem. Phys*., 2000, **112**, 1541-1546. (b) V. Duzhko, A. Semyonov, R. J. Twieg, K. D. Singer, *Phys. Rev. B*, 2006, **73**, 064201. (c) I. Shiyanovskaya, K. D. Singer, R. J. Twieg, L. Sukhomlimova, V. Gettwert, *Phys. Rev. E*, 2002, **65**, 041715. (d) T. Kreouzis, K. J. Donovan, N. Boden, R. J. Bushby, O. R. Lozman, Q. Liu, *J. Chem. Phys*., 2001, **114**, 1797-1802. (e) V. Lemaur, D. A. da Silva Filho, V. Coropceanu, M. Lehmann, Y. Geerts, J. Piris, M. G. Debije, A. M. van de Craats, K. Senthilkumar, L. D. A Siebbeles, J. M. Warman, Jean-Luc Brédas, J. Cornil, *J. Am. Chem. Soc*., 2004, **126**, 3271–3279.

19 (a) I. Bleyl, C. Erdelen, H.-W. Schmidt, D. Haarer, *Philos. Mag. B*, 1999, **79**, 463–475; (b) H. Iino, J. Hanna, R. J. Bushby, B. Movaghar, B. J. Whitaker, *J. Appl. Phys*., 2006, **100**, 043716; (c) M. Funahashi, F. Zhang, N. Tamaoki, J. Hanna, *ChemPhysChem*, 2008, **9**, 1465–1473; (d) S. R. Farrar, A. E. A. Contoret, M. O'Neill, J. E. Nicholls, G. J. Richards, S. M. Kelly, *Phys. Rev. B*, 2002, **66**, 125107.

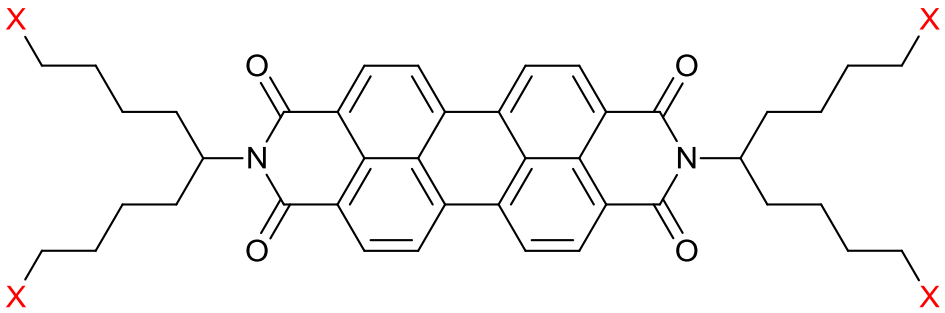

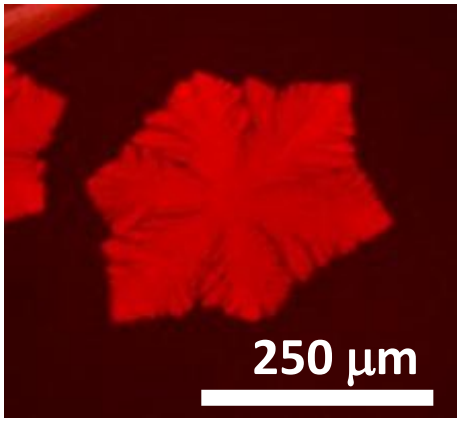

X =

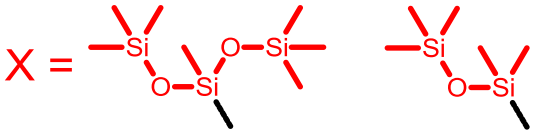

X =

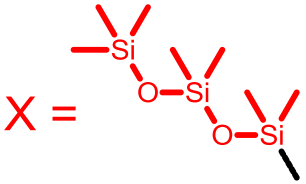

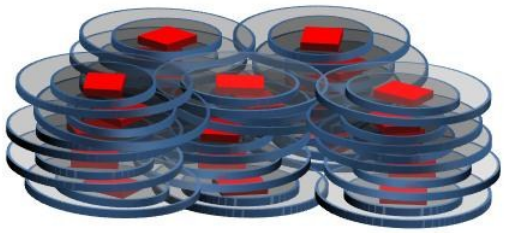

X =

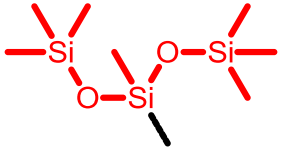

Ordered columnar phase

μ_e ~ 1x10^{-1} cm^{2}V^{-1}s^{-1}

Disordered columnar phase

μ_e ~ 1x10^{-3} cm^{2}V^{-1}s^{-1}